

DOE/NV/10872--T259

# FINAL REPORT

TO

US DOE YMSCO

FROM

HEAT TRANSFER LABORATORY  
MECHANICAL ENGINEERING DEPARTMENT  
UNIVERSITY OF NEVADA, LAS VEGAS

## "HEAT TRANSFER STUDIES"

R. BOEHM, PI  
Y. -T. CHEN, CO-PI

# MASTER

APRIL 12, 1996

DISTRIBUTION OF THIS DOCUMENT IS UNLIMITED

*UK*

## Introduction

Many simple (without thermal effects) ground-water flow models have been used for analysis of water resource problems since the 1960's. The emphasis on more complicated ground-water flow models began to shift with the focus on waste management problems during the 1970's. This shift in emphasis was largely brought about by site selection activities for geologic repositories for disposal of high-level radioactive wastes.

Several model developments during the 1970's and well into the 1980's focused primarily on saturated ground-water flow because geologic repositories in salt, basalt, granite, shale, and tuff were envisioned to be below the water table. The ground-water flow model development has shifted to unsaturated flow models because the unsaturated zone at Yucca Mountain was selected as a potential high-level radioactive waste disposal site. This emphasis was underlined by the Nuclear Waste Policy Amendment in 1987 which selected Yucca Mountain as the only site under investigation for potential disposal of high-level radioactive waste.

Many unsaturated flow models have been developed and used since the mid-1980's. A few unsaturated flow models have also been developed in the 1990's. These models with associated submodels found their origins in university, national laboratory, and private company work. Most of the existing models have a considerable amount of similarity.

Under the U.S. Department of Energy (DOE), the Civilian Radioactive Waste Management System Management and Operating Contractor (CRWMS M&O) has the responsibility to review, evaluate, and document the existing computer models; to conduct performance assessments; and to develop performance assessment models, where necessary. Two major regulatory requirements are the main criteria for selection of ground-water flow models in the unsaturated zone. One is of calculating the pre-emplacement ground-water travel time (10 CFR 60), and another is of calculating the release of radionuclides to the accessible environment over 10,000 years (40 CFR 191). The thermal energy impact from the decaying waste plays an important role for a detailed analysis of unsaturated flow under repository conditions. Thus it is important to understand how significant is the impact of thermal energy from the spent fuel on the possible release of radionuclides to the environment.

Two issues are apparent. The thermal effects from the fuel can cause convective flows in the surrounding formation. These flows can then bring moisture from a lower-lying saturated zone. Effects of the heating can also modify

the flows of episodic water from the surface. A second issue is the possibly penetration of moisture that exists in close proximity (for the reasons just outlined) into the storage area. Moisture penetration in some form into the area where fuel is stored is virtually certain, and some estimates of the magnitude of moisture penetration are needed.

Our work over the many months of this project has focussed on a number of issues. Initially we were concerned with various types of visualization techniques. Porous media problems are particularly difficult to visualize. We have applied the Christiansen Cell approach and the use of hygroscopic materials. We were partially successful before programmatic changes made it desirable for us to focus on other problems.

Then we moved toward experiments that could have more application quantitatively. We identified the lack of calibration data for numerical modelers to be a significant shortcoming of the current state of performance prediction for a waste repository. In fact we became aware of the problems of trying to predict humidity in enclosed spaces in a porous formation. Experiments were then designed to quantify the effects of various parameters on humidities measured in these kinds of spaces. Part of this work focused on episodic water flows in heated formations, and another part involved the drying of residually saturated porous formation.

A large number of studies are summarized here. These are given roughly in the opposite order that they are discussed in the two paragraphs above. Details of the data are, in general, not given. Instead information is furnished for the interested reader to find this information in our quarterly reports given throughout the project.

## **I. A Study of the Extension of Multi-Phase Models to Sub-Residual Saturation**

### **(1) Introductory comments**

YMSCP have recently indicated an important concern that the results of the previous thermal-hydrologic calculations may have some deficiencies based on the current understanding of the physical processes occurring in the drift at elevated temperatures and subresidual liquid saturations. They have found that the numerical modelers have used a modified capillary pressure function to fix arbitrarily the maximum capillary pressure for subresidual saturations. In doing this, the numerical modelers have used certain computational procedures to interpolate the liquid saturations ranging from 0 to residual saturations in numerical codes such as TOUGH and FEHM in order to avert numerical

convergence problems. It has been shown that this assumption may not represent very well the real conditions in the near-field of the high-level radioactive nuclear waste repository due to a high thermal load from the waste packages.

In the Yucca Mountain Site Characterization Plan, the writers apparently believed that strong capillary forces can draw water into the pores of unsaturated rock. They believed that water travels slowly in the unsaturated rock if water is confined to the pores. They also believed that the capillary forces would keep water from dripping into the repository. The assumption has been made that water will eventually get into the repository, dissolve radionuclides, and reenter the flow in the mountain. However, it was assumed that it will take tens of thousands of years for the water to travel from the repository to the accessible environment in significant quantities.

In the natural state, it is known that varying quantities of water can reside in underground rocks due to differences in their porous structure. Without a heated condition in the underground, the residual water in the rock can penetrate downward to the water table and can be recharged from episodic water flows from surface. The residual water may stay there for many days, months, or years due to the capillary force equilibrium in the porous medium.

It is well understood, though, that the capillary forces in rock structures can be easily changed in high temperature environments. When the capillary force decreases at high temperatures in the porous medium, the speed of water flow through the medium can then be accelerated. The high thermal load from buried high-level radioactive spent nuclear fuel can easily heat water in the near-field of the repository above the boiling temperature.

We were interested in investigating the multi-phase flow models as they apply to sub-residual saturation conditions in the porous medium under various thermal boundary conditions. The surface tension of water decreases when the temperature increases. As a consequence, the capillary pressure, which can build up the flow resistance in the porous medium, will be significantly reduced at high temperature conditions compared to what is found at lower temperatures. This will obviously result in higher liquid flows in the porous medium which could cause more moisture to penetrate into the repository. At high temperatures, the water will not be easily confined to the pores due to the increased internal energy. In contrast, water can be easily evaporated, and it can travel in the porous medium and any fractures present due to the strong driving force from the pressure gradients.

It is of interest to find out how fast the residual water can be evaporated into a gas flow through a heated porous medium initially at residual saturation. Analysis of this effect also allows the determination of the levels of relative humidity that exist in adjacent spaces. Flow modelers can easily make inaccurate predictions of the humidity values from their current numerical modeling calculations related to the underground storage environment. The modelers have assumed the capillary pressures to be a maximum value to determine the humidity levels in the high-level nuclear waste repository design. This error can have a very negative impact on the corrosion predictions that follow from that. Evaporation due to the high temperatures can also have an erroneous impact on the results. The capillary pressure within the porous medium will be reduced when the evaporation takes place there. Therefore, more water (liquid and vapor) may penetrate into the repository which can result in a higher humidity level in the vicinity of the waste package and drift than shown by previous calculations. Possible corrosion rates can be greatly increased as a result of this.

To attempt to understand water-penetration issues, our studies were focused on the limitations of applying multi-phase flow models to the hydrothermal processes occurring when the liquid saturation falls below residual levels. Our primary objective has been to produce experimental data that will be of value to numerical modelers involved in repository design.

## (2) Design of drying experiments

An experimental program in our laboratory analyzed drying effects of residue water in a porous media with a heated boundary on the test section. The experimental setup is shown in Figure 1. The detailed test section schematic diagram is shown in Figure 2.

In one set of experiments two flow rates, high and low, of nitrogen gas with an isothermal boundary condition have been used, and in another set, a high flow rate of the same gas with an adiabatic boundary condition has been applied. One condition started with flowing nitrogen gas through the test section and simultaneously heating up the porous medium at the same time (denoted in what follows as the "transient heating case"). The other condition started initially with heating up the porous medium with no flow, and then running the nitrogen gas flow through the test section after a steady-state temperature distribution had been reached (denoted in what follows as the "steady heating case").

The test section has been constructed of a 2'-long plastic tube that has an inside diameter of 2". The test section has also constructed of a 16" long aluminum cylinder that has an inside diameter of 1.5" and two windows (0.275" x 5.625"). The reason why aluminum was chosen for this application is because this material is rust resistant and it has a high thermal conductivity. Nitrogen gas has been used as a displacing fluid and water was the displaced fluid in the glass beads. Several different mass flow rates of nitrogen gas with or without heating effect were studied. Various heating environments were studied later in the work. The mass flow rate of nitrogen gas is controlled by a servo valve/feedback control system. The data of mass flow rate are recorded using digital signal conditioning and data acquisition devices. Tests begin at the residual saturation condition and continue until steady-state conditions are reached, which may or may not find a completely dried porous medium.

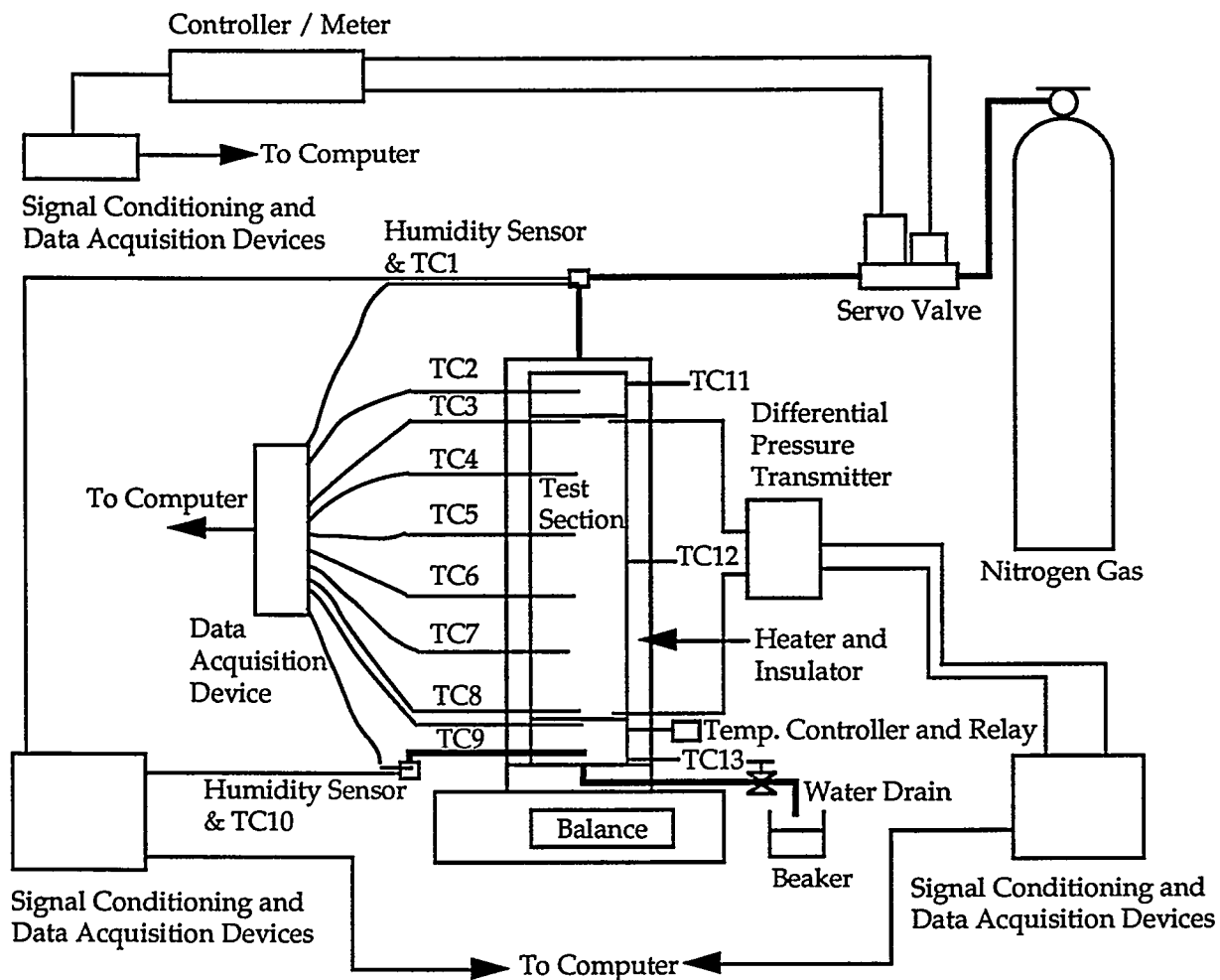


Figure 1. Diagram of piping and instrumentation used in the drying experiment.

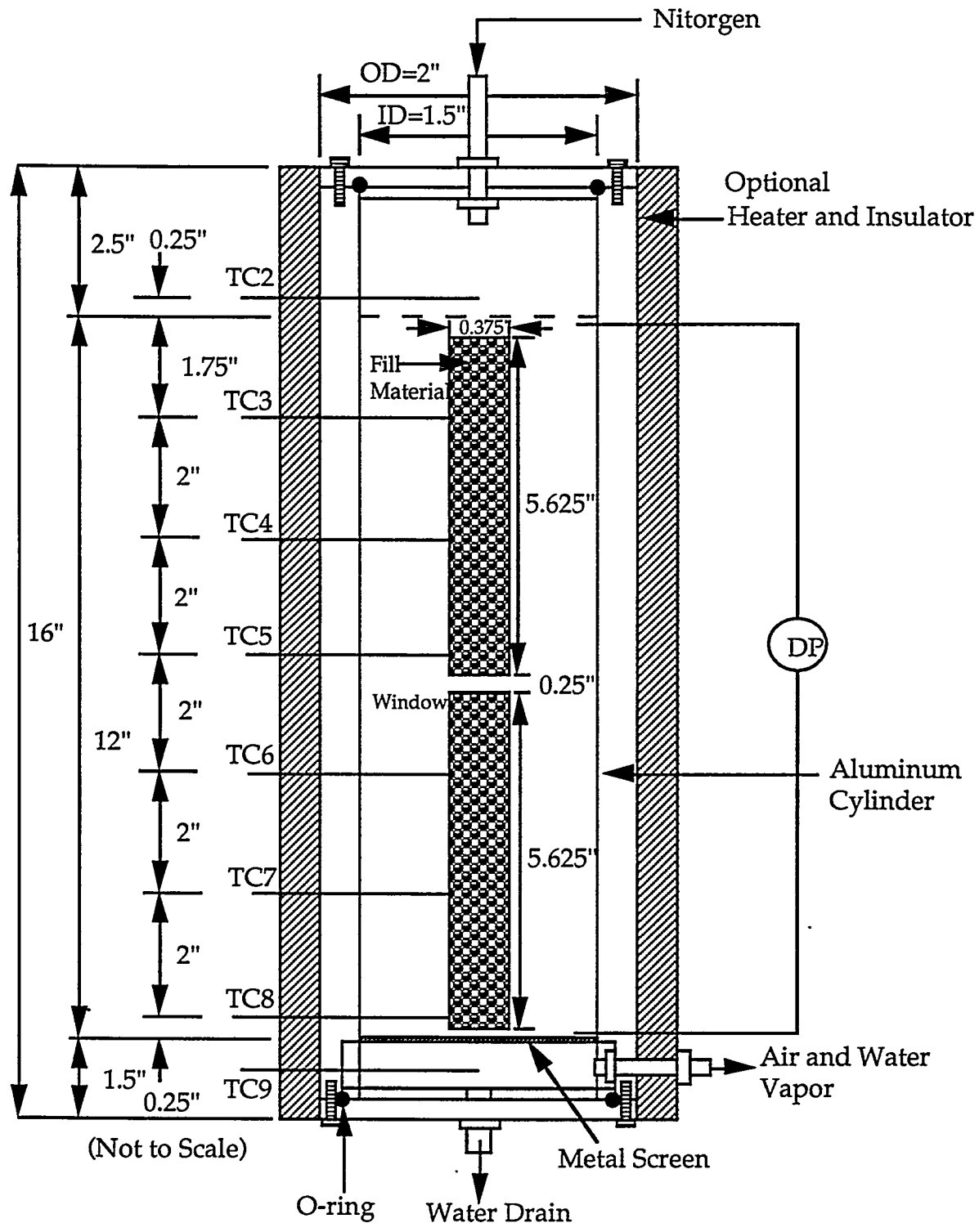


Figure 2. Schematic diagram of the test section used in the drying experiments. Two windows on one side allow visual observations during the test runs. The test section can be operated with or without heating.

Quartz beads with an average diameter of 0.037" are used as the fill material in the test section. Industrial grade nitrogen gas was used as the displacing fluid and water was the displaced fluid in the glass beads. Two gas flow rates of 1 and 0.5 SLPM were used in the studies reported here. In this case, the mass flow rates of nitrogen gas yield  $Re=0.868$  and  $Re=0.434$ , respectively. These Reynolds numbers assure that the flows were in the Darcy region. A mass flow controller with a servo valve has been used to control the nitrogen gas mass flow rate to flow through the test section. It has  $\pm 1\%$  accuracy on the full range of 5 SLPM. From the initial test results, a smaller valve was needed for better accuracy results so the control valve has been changed to a capacity of 1 SLPM. Distilled water has been used to avoid any interferences such as any chemical bonding strength that might be caused by impurities.

Two capacitance humidity sensors have been used to measure the inlet and outlet humidities from the test section. These sensors have about  $\pm 1\%$  accuracy, based on the full range measurement. (It was found that these were quite fragile, and not suitable for applications over several runs. Others may be more appropriate from this standpoint.) These humidity sensors have been calibrated using the ASTM E104-85, which is a standard practice for maintaining constant relative humidity by means of aqueous solutions. Three different kinds of chemicals, lithium chloride with a low range of humidity values, sodium chloride with a moderate range of humidity values, and potassium sulfate with a high range of humidity values have been used. Three temperature dependent calibration tests have been studied. The highest temperature listed in the ASTM E104-85 is 50 °C. Thus, a calibration with a higher temperature close to the boiling point of water is not available. During the tests, the output capacitance of the humidity sensors has been converted to the voltage. These were recorded as a function of time.

A total of thirteen 30 gauge K-type thermocouples have been used in the test section to measure the temperatures with a maximum of 0.75% error. These were placed at several locations within the test section. Three thermocouples were located on the top, middle, and bottom outside of the test section to assess the accuracy of the assumed isothermal boundary condition on the wall. A case where a heated wall has been used on the experiment has been reported. An Omega 1" x 8" heating tape (maximum output rating of 8.6 W/in<sup>2</sup>) has been chosen to accomplish the heating task. An on-off type solid state temperature controller has been used to control the heating temperature.

Pressure drop through the test section was measured with a differential pressure transmitter with 5" water maximum range and  $\pm 1\%$  accuracy. A smaller range of 0.5" water of differential pressure transmitter was also used later for the small mass flow rates. The output voltages from the transmitter have been recorded.

Weight readings of the entire test section with respect to time have also been recorded during the test, and these were accomplished with a digital balance. Comparisons are made between the change of water content in the test section inferred from integration of the mass flow of water out (estimated from the air mass flow and humidity measurements) with readings taken from the digital balance. A digital balance of 12 kilogram capacity, a 0.1 gram readability, and  $\pm 1\%$  accuracy has been used to measure the weight of the test section as a function of time.

Room temperature and atmospheric pressure have also been measured. A computer with a LabVIEW data acquisition system has been used to collect all data from the experiment.

### **(3) Results for $Re=0.868$ with a transient heated boundary condition**

This test began with the system at residual saturation. At the start of the experiment, the nitrogen flow and the wall heater were turned on simultaneously. The nitrogen gas volumetric flow rate used was 1 SLPM. A 16" long aluminum cylinder that has an inside diameter of 1.5" and two windows (0.275" x 5.625") was used in this experiment. Data were reported from the starting condition.

All of results for the transient heating case with a 90°C wall set point have been reported in the quarterly report<sup>1</sup> dated January 19, 1996 to validate the results on a slightly different Reynolds number ( $Re=0.8672$ ) which have been reported in the quarterly report dated October 20, 1995. These results include the relative humidity variations at the inlet and the outlet of the test section vs. time, the amount of water transported from the experiment compared from estimates using humidity measurements and digital balance measurements, the volumetric flow rate of nitrogen gas, and pressure drop across the porous medium vs. time, nitrogen gas inlet and outlet temperatures vs. time, temperatures at thermocouples at various locations inside the test section vs. time, and temperatures of the top, middle, and bottom wall vs. time.

---

<sup>1</sup>Any reference to a "quarterly report" denotes a report submitted earlier by our group to DOE. The specific date is indicated for possible access. These should be on file at DOE YMSCO.

#### **(4) Results for Re=0.434 with a steady heated isothermal boundary condition**

This test also began with the system at residual saturation. At the start of the experiment, the wall heater was turned on to heat up the porous medium. When a steady-state temperature distribution was reached, the nitrogen gas flow then was allowed to run through the test section. The nitrogen gas volumetric flow rate used was 0.5 SLPM. A 16" long aluminum cylinder that has an inside diameter of 1.5" and two windows (0.275" x 5.625") was used in this experiment. Data were reported from this starting condition.

All results for the steady heating case with a 90°C wall set point have been reported in the quarterly report dated January 19, 1996. These include the relative humidity variations at the inlet and the outlet of the test section vs. time, the amount of water transported from the experiment was compared from estimates using humidity measurements and digital balance measurements, the volumetric flow rate of nitrogen gas and pressure drop across the porous medium vs. time, nitrogen gas inlet and outlet temperatures vs. time, temperatures of the thermocouples inside test section vs. time, and temperatures of the top, middle, and bottom wall vs. time.

#### **(5) Results for Re=0.8675 with an isothermal boundary condition**

This test also began with the system at residual saturation. At the start of the experiment, the wall temperature was maintained at the room temperature. The nitrogen gas volumetric flow rate used was 1 SLPM. A 16" long aluminum cylinder that has an inside diameter of 1.5" and two windows (0.275" x 5.625") were used in this experiment. Data were reported from this starting condition.

All of results for this isothermal boundary condition test have been reported in the quarterly report dated July 20, 1996. These include the relative humidity variations at the inlet and the outlet of the test section vs. time, the amount of water transported from the experiment was compared from estimates using humidity measurements and digital balance measurements, room temperature vs. time, nitrogen gas inlet and outlet temperatures vs. time, and temperatures at thermocouples inside test section vs. time.

#### **(6) Results for Re=0.434 with an isothermal boundary condition**

This test also began with the system at residual saturation. At the start of the experiment, the wall temperature was maintained at the room temperature. The nitrogen gas volumetric flow rate used was 0.5 SLPM. A 16" long aluminum

cylinder that has an inside diameter of 1.5" and two windows (0.275" x 5.625") was used in this experiment. Data were reported from this starting condition.

All results for this isothermal boundary condition test have been reported in the quarterly report dated July 20, 1996. These include the relative humidity variations at the inlet and the outlet of the test section vs. time, the amount of water transported from the experiment comparing estimates using humidity measurements and digital balance measurements, room temperature vs. time, nitrogen gas inlet and outlet temperatures vs. time, and temperatures at various thermocouples inside the test section vs. time.

#### **(7) Results for $Re=0.046$ with an isothermal boundary condition**

This test also began with the system at residual saturation. At the start of the experiment, the wall temperature was maintained at the room temperature. The nitrogen gas volumetric flow rate used was 0.05 SLPM. A 2'-long plastic tube that has an inside diameter of 2" was used in this experiment. Data were reported from this starting condition.

All of results for this isothermal boundary condition test have been reported in the quarterly report dated on July 20, 1996. These include relative humidity variations at the inlet and the outlet of the test section vs. time, the amount of water transported from the experiment versus time from estimates using humidity measurements and digital balance measurements, room temperature vs. time, nitrogen gas inlet and outlet temperatures vs. time, and temperatures at various thermocouple locations inside the test section vs. time.

#### **(8) Results for $Re=0.876$ with an adiabatic boundary condition**

This test also began with the system at residual saturation. At the start of the experiment, the wall temperature was maintained at the room temperature. The nitrogen gas volumetric flow rate used was 1.0 SLPM. A 2'-long plastic tube that has an inside diameter of 2" was used in this experiment. Data were reported from this starting condition.

All of results for this isothermal boundary condition test have been reported in the quarterly report dated July 20, 1996. These include the relative humidity variations at the inlet and the outlet of the test section vs. time, the amount of water transported from the experiment from estimates using humidity measurements and digital balance measurements, room temperature vs. time, nitrogen gas inlet

and outlet temperatures vs. time, and temperatures at various thermocouples the inside test section vs. time.

**(9) The theoretical study**

A theoretical study has also been initiated in an attempt to supplement the insights gained from the experiments. The approach taken was to assume a one-dimensional transient system in which a two-component (condensable and noncondensable) gas mixture flows through a porous medium with evaporation. In order to predict properly the various phenomena that affect the drying, it was desirable that restrictive conditions imposed on the formulation be minimized. Three continuity equations (i.e., for nitrogen, water vapor, and condensed liquid) and two energy equations (i.e., for gas mixture, and condensed liquid and porous medium) were used. To make these equations manageable, the following assumptions were introduced: (1) The porous medium is homogeneous. (2) The streamwise mass diffusion is negligible compared to that of convective transport. (3) The total pressure in the porous medium is constant. (4) All the thermophysical properties except the nitrogen gas and water vapor densities were taken as constant.

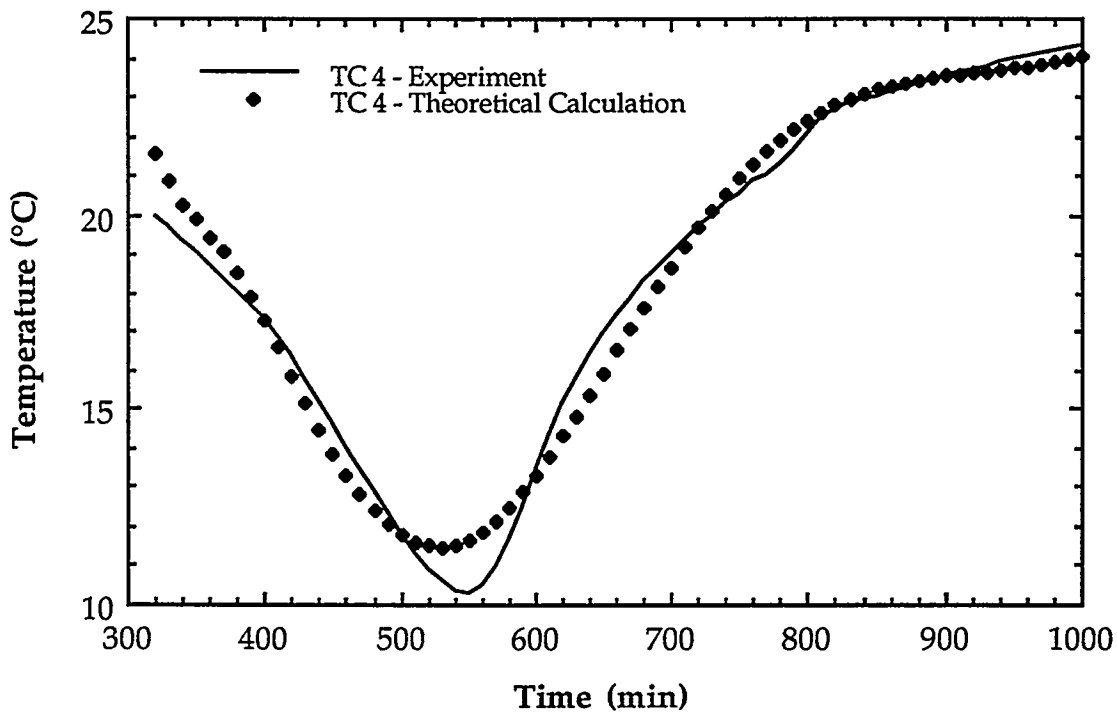


Figure 3. The temperature comparison between a theoretical calculation and experimental results.

Figure 3 shows the one-dimensional comparison between the experimental result and the theoretical calculation at the location of thermocouple 4 in the porous media. A maximum 15% discrepancy between two results is seen. The theoretical calculation result shows that the evaporation initiates earlier and lasts a little longer than the experimental result indicate. This may be due to the imprecision in predicting that mass transfer coefficient.

### **(10) Summary Comments**

We have explored a variety of drying conditions in porous media and the resulting humidity conditions of the drying gas. Our studies of computational methods used in current numerical codes for determining performance estimates show that humidity values can easily be underpredicted in sub-residually saturated conditions. We suggest that capillary pressures should be carefully examined under various boundary conditions, and especially at elevated temperatures. In the past, the capillary pressures have been arbitrarily fixed to a maximum value by computer modelers to avoid numerical divergence problems.

## **II. A Study of Unsaturated Flows with Heat Transfer in a Repository Drift**

Complicated and coupled thermal-hydrological transport phenomena in the near field and within the drift environment of the repository are generated as a result of the thermal load. The water flow and vapor presence need to be extremely well characterized in the near field and drift of the nuclear waste repository. This is needed to understand possible moisture transport paths that could result in penetration of water vapor to the waste. This information, in turn, is needed to understand the moisture environment (humidity or presence of liquid water) around the waste packages to use in the waste-package design process to control corrosion. This is being addressed by extensive use of computer models of the flow phenomena. There was a lack of experimental data to substantiate the modeling results.

Our work was an attempt to begin to rectify this problem as well as to provide experimental insights to flow phenomena in this type of system. The purpose of this experimental study was to investigate a certain class of thermal-hydrological phenomena in unsaturated porous media. The scale and complexity of the Yucca Mountain Site result in a physical situation that is impossible to duplicate in any kind of controlled experiments. As a result, there is no claim made that our experiments represent an exact analog to the physical situation. Our main

contribution is to provide numerical modelers the relevant data with a controlled set of boundary conditions. This work has been focused on response near the heater and in the annulus.

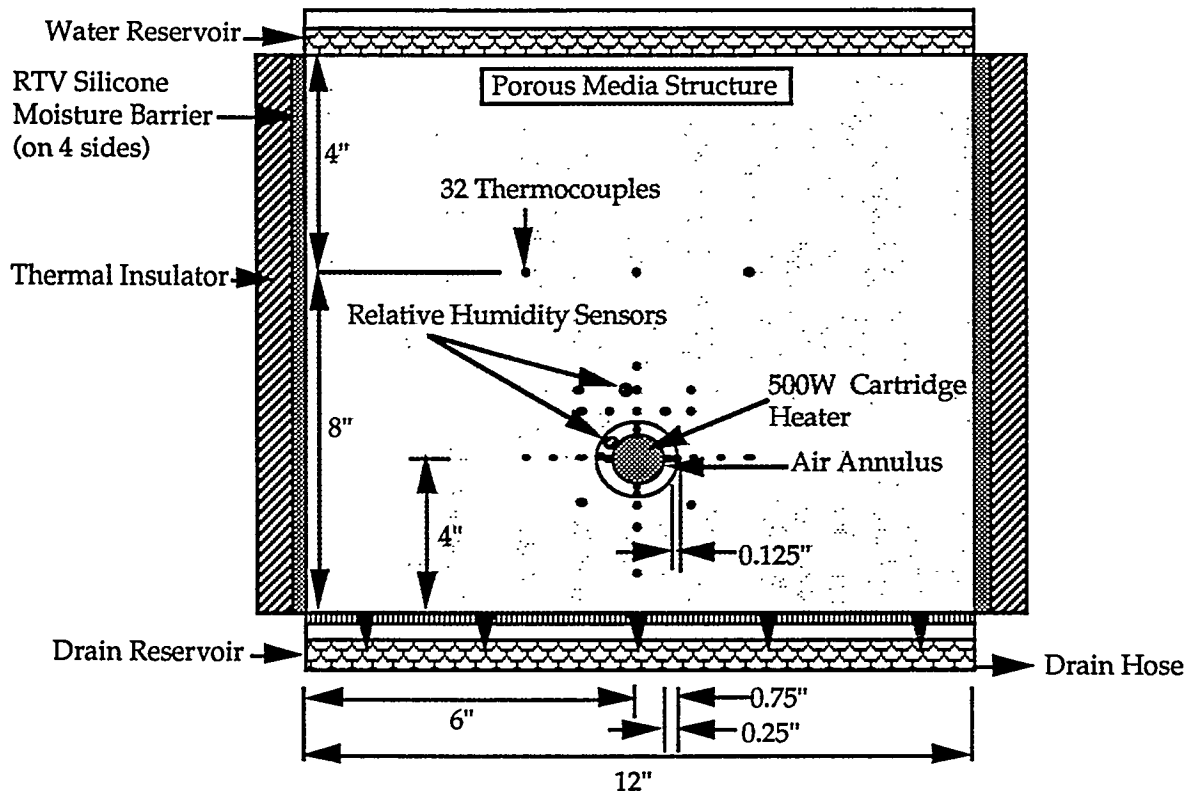


Figure 4. A front-view schematic of the experimental setup to simulate some aspects of flows around an underground repository. The dimension into the page is 1.5 in.

Figure 4 shows the test section of the experiments using a rigid porous medium 38.1 mm x 304.8 mm x 304.8 mm (high) (1.5 in x 12 in x 12 in) which was prepared with a 38.1 mm (1.5 in) hole through the thin dimension. The rigid porous structure is made by Eaton Products International Company. In the manufacture of this material, tiny, precisely-sized spherical particles are bonded together to form rigid three-dimensional shapes that have an evenly distributed network of interstitial pores which are of uniform size, completely open and interconnected. A sample of specific properties was used throughout all of our work. The void volume of the porous media structure used in this work is 30%. The bulk density is 1.6 grams/cc, the permeability is  $5.15 \times 10^{-6}$  sq mm ( $5.54 \times 10^{-11}$  sq ft), and the coefficient of thermal expansion is  $1.08 \times 10^{-7}$  in/in/ $^{\circ}$ C. The combination

of relatively high porosity and small physical size results in short times for moisture travel through the test section.

A 25.4 mm (1 in) diameter and 38.1 mm (1.5 in) long 500 W electrical cartridge heater was installed horizontally through the rigid, porous medium, forming an annulus in the hole. The heater temperature was maintained essentially at a constant value using a time-proportional variable set-point controller on a constant heater temperature case. A variable voltage transformer was used to control the constant heat flux case. A ceramic material was used to seal both sides of the annulus and to support the heater in the annulus. This seal reduces the heat loss and prevents steam from escaping from the side walls. The four sides except top and bottom of the porous medium were then coated with a high temperature silicone sealant so that moisture could not escape through those surfaces. A 50 mm thick polyurethane material was used as an insulator on the four sides of the porous medium but not the top and bottom surfaces.

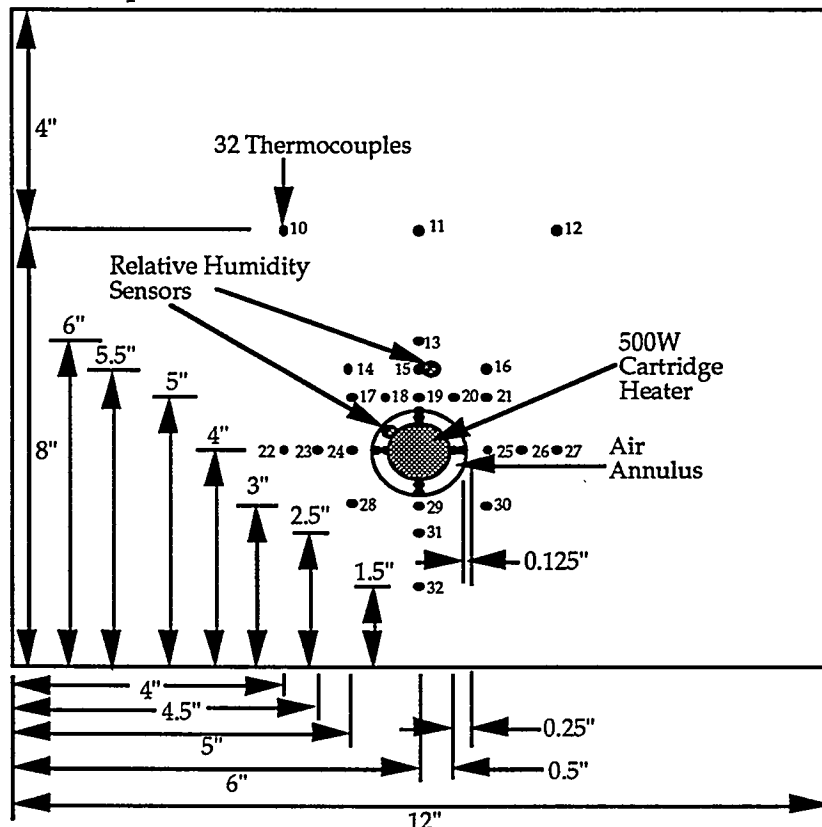


Figure 5. Schematic location of the thermocouples and humidity sensors in the repository flow experiments.

Figure 5 shows nine and twenty-three 30 gauge K-type thermocouples that were used to measure the temperatures in the annulus and the porous media

structure, respectively. The calibrated thermocouples were inserted from one of the large surfaces of the test section and penetrated approximately half way through the small dimension of the block.

A commercial capacitance-type sensor was used to measure the relative humidity in the annulus, and a single measurement location was assumed to give representative readings of the conditions there. The sensor has an operating temperature range from -40 to 180°C and an accuracy of  $\pm 1\%$  of the full scale reading. After calibration it was inserted through the ceramic to the inside wall of the annulus. At this location the highest temperature experienced in these experiments was below 180°C.

Data logging was accomplished with a personal computer with a LabVIEW data acquisition system. The data were recorded every 10 seconds.

An experimental run was initiated with a dry porous material with a steady-state temperature distribution characterized by a desired heater temperature. A known amount of water at ambient temperature was then introduced at the top of the porous medium.

The configuration just described has the following boundary conditions: All sides were insulated and impenetrable to moisture. The top and bottom were open to atmospheric conditions. Water was allowed to flow from the top to the bottom of the experiment. A constant temperature or constant heat flux, horizontally-mounted heater is located in an annulus.

Analysis of several experiments showed that the temperature response of a block of material is symmetrical around a vertical center line through the axis of the heater. Hence only results for one half (the left hand side) of the experiment have been reported. A focus of the experiments was to examine temperature responses to the water flow within the porous material, particularly near the heater annulus. Also of interest was the time variation of relative humidity within the annulus. The effects of water quantity on the response of the constant heater temperature system and constant heat flux system have been investigated.

### **(1) Low constant heat flux with 300 ml water**

An experimental run began with a dry porous material and a low constant heat flux (i.e. 14.5 V and 0.46 A) on the heater. In this report, studies of a constant heat flux condition have been reported that yield a low heater temperature ( $\approx 150^\circ\text{C}$ ) in the dry condition. Tap water at ambient temperature is introduced from the top of the porous medium when a steady state dry condition in the porous medium and

air annulus was reached. With constant heat flux conditions, the heater temperature did not remain constant when water and/or vapor penetrates into the air annulus. Experiment was performed using 300 ml water being poured onto the top of the 12" x 1.5" surface.

All results for this experiment have been reported in the quarterly report dated October 20, 1995. These include the variations of temperature and relative humidity in the air annulus, the variations of temperature at a 3", 5", 5.5", and 8" height in the porous medium, the variations of temperature at the left hand side of annulus, and the variations of temperature at a vertical top and bottom the porous medium.

### **(2) Low constant heat flux with 200 ml water**

An experimental run began with a dry porous material and a low constant heat flux (i.e. 14.5 V and 0.46 A) on the heater. Studies have been reported of a constant heat flux condition that yields a low heater temperature ( $\approx 150^{\circ}\text{C}$ ) in the dry condition. Tap water at ambient temperature is introduced from the top of the porous medium when a steady state dry condition in the porous medium and air annulus was reached. Experiments were performed examining the response in the porous medium to 200 ml of water being poured onto the top of the 12" x 1.5" surface.

All results for this experiment have been reported in the quarterly report dated October 20, 1995. These include the variations of temperature and relative humidity in the annulus, the variations of temperature at a 3", 5", 5.5", and 8" height in the porous medium, the variations of temperature at the left hand side of annulus, and the variations of temperature along a vertical line in the porous medium.

### **(3) High constant heat flux with 200 ml water**

An experimental run began with a dry porous material and a low constant heat flux (i.e. 20.2 V and 0.64 A) on the heater. Studies have been reported of a constant heat flux condition that yields a high heater temperature ( $\approx 238^{\circ}\text{C}$ ) in the dry condition. Tap water at ambient temperature is introduced from the top of the porous medium when a steady-state dry condition in the porous medium and air annulus was reached. With constant heat flux conditions, the heater temperature did not remain constant when water and/or vapor penetrates into the air annulus.

Experiments were performed examining the response in the porous medium to 200 ml of water being poured onto the top of the 12" x 1.5" surface.

All results for this experiment were reported in the quarterly report dated April 20, 1995. These include the variations of temperature and relative humidity in the annulus, and variations of temperature at a variety of locations within the porous medium.

#### **(4) High constant heater temperature with 200 ml water**

An experimental run began with a dry porous material and a constant heater temperature 238°C. Tap water at ambient temperature was introduced from the top of the porous medium when a steady state dry condition in the porous medium and air annulus was reached. With constant heater temperature conditions, the heater temperature drastically increased when water and/or vapor penetrated into the annulus. This is due to the surface temperature of heater being cooled off by the saturated steam and the on-off type temperature controller supplying increased power to the heater to try to maintain the constant temperature at the set point. The control thermocouple was attached to the surface of heater. It resulted in an over-compensating effect. Experiments were performed examining the response in the porous medium to 200 ml of water being poured onto the top of the 12" x 1.5" surface.

All of the results from this experiment were reported in the quarterly report dated January 20, 1995. These include the variations of temperature and relative humidity in the annulus, and the variations of temperature at a variety of locations within the porous medium.

#### **(5) Low constant heater temperature with 200 ml water**

An experimental run began with a dry porous material and a constant heater temperature of 110°C. Tap water at ambient temperature was introduced from the top of the porous medium when a steady-state dry condition in the porous medium and annulus was reached. This case showed an increase in heater temperature as a response to the moisture penetrating the annulus, but to a lesser degree than that of the case described above. Experiments were performed examining the response in the porous medium to 200 ml of water being poured onto the top of the 12" x 1.5" surface.

All of results for this experiment were reported in the quarterly report dated January 20, 1995. These include the variations of temperature and relative humidity

in the annulus, and the variations of temperature at a variety of locations within the porous medium.

#### **(6) High constant heater temperature with 300 ml water**

An experimental run began with a dry porous material and a constant heater temperature 238°C. Tap water at ambient temperature was introduced from the top of the porous medium when a steady state dry condition in the porous medium and air annulus was reached. A response in heater temperature similar to that described in Section (4) above was seen. Experiments were performed examining the response in the porous medium to 200 ml of water being poured onto the top of the 12" x 1.5" surface.

All of the results from this experiment were reported in the quarterly report dated January 20, 1995. These include the variations of temperature and relative humidity in the annulus, and the variations of temperature at a variety of locations within the porous medium.

#### **(7) Low constant heater temperature with 300 ml water**

Similar comments to those made above in section (5) hold here, but a greater amount of water was introduced in this case. Detailed results were also reported in the January 20, 1995 report.

### **III. Unsaturated Flow and Heat Transfer Experiments with Moisture Migration**

We carried out experiments that focused on investigations of response of the field some distance from the heat source as a result of the introduction of an episodic water flow. There are two fundamental differences between this work and that just described. In this work, the far-field response was examined in detail (rather than the near field), and a loose fill of glass beads was used (rather than a rigid porous medium).

A schematic of the experimental apparatus is shown in Figure 6. A horizontally mounted 1000 W electrical cartridge heater was located 10.2 cm (4 inch) from the bottom of the medium spanning the tank (15.24 cm). The whole assembly was heated in the dry condition until the initial temperature of the heater was about 270°C. Water at room temperature was then introduced to the top of the medium in a spatially uniform manner. The energy transport in such a medium occurred by conduction in all of the phases as well as by convection in those phases which were able to move.

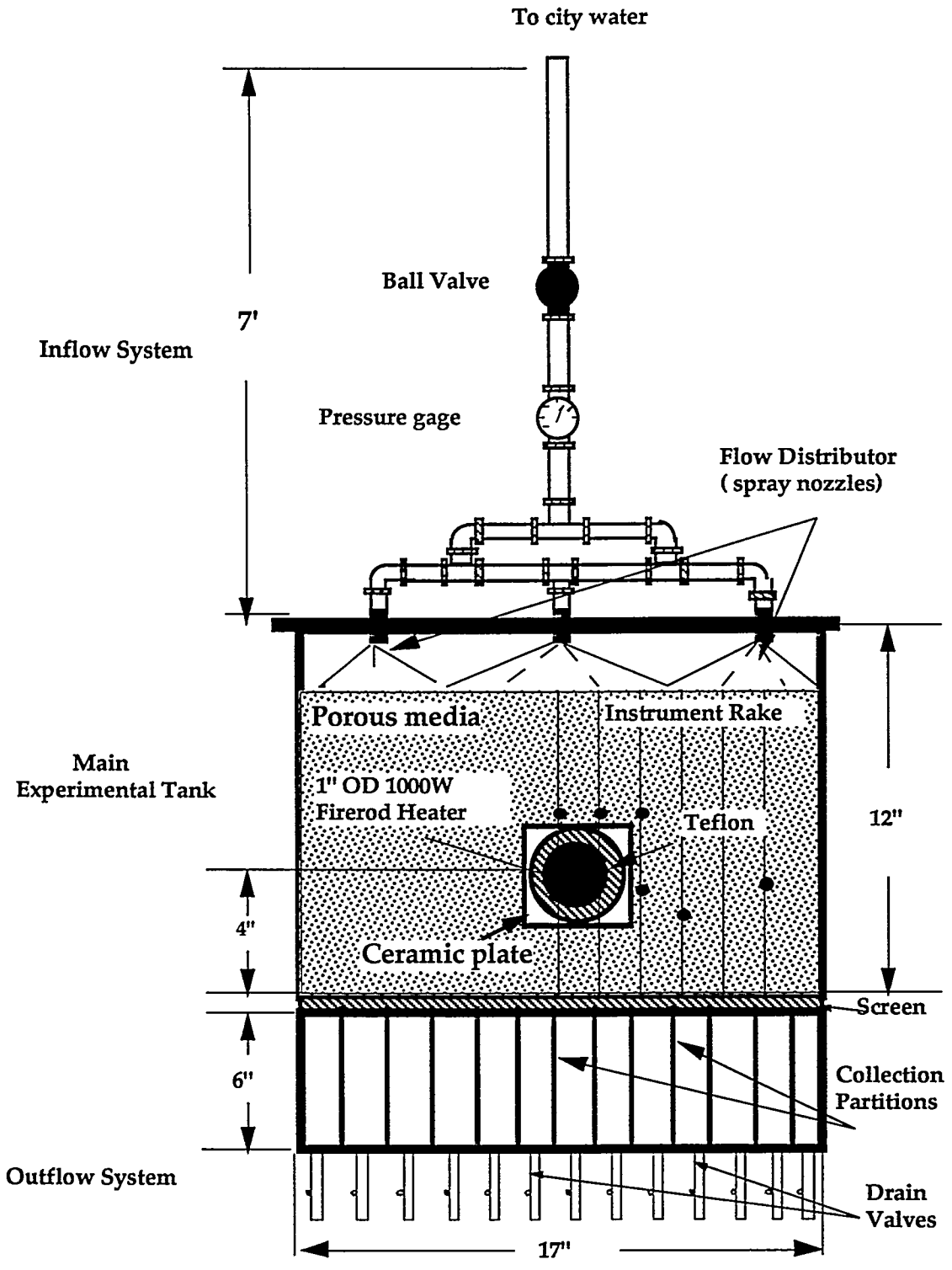
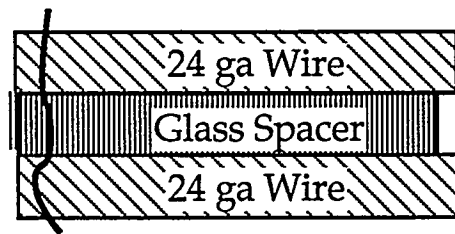
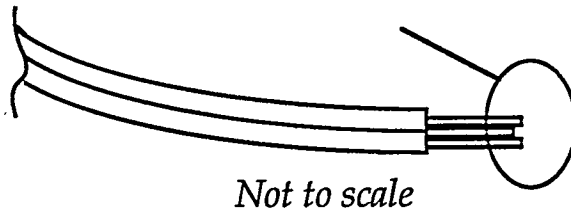
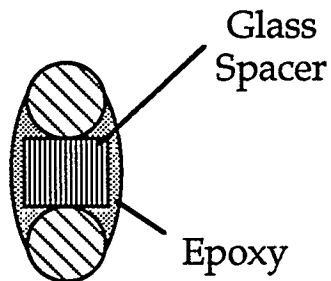


Figure 6. Sketch of the modified experimental apparatus system (not to scale).

Detail  
Shown  
Below



Side View



End View

Figure 7. Design of the capacitance elements used for determining moisture content.

Capacitance elements were developed in our laboratory for mapping moisture presence throughout the apparatus (Figure 7). The idea for this sensor was to detect the presence of water through a change in capacitance of the experiment media. The elements were made from simple duplex 24 gauge (0.056 inch) solid

conductor wire. The tips on one end were stripped of insulation and the two wires epoxied on each side of a small dielectric spacer as shown in the figure. Six of these capacitance element probes were built. The placement of these devices is shown in Figure 8.

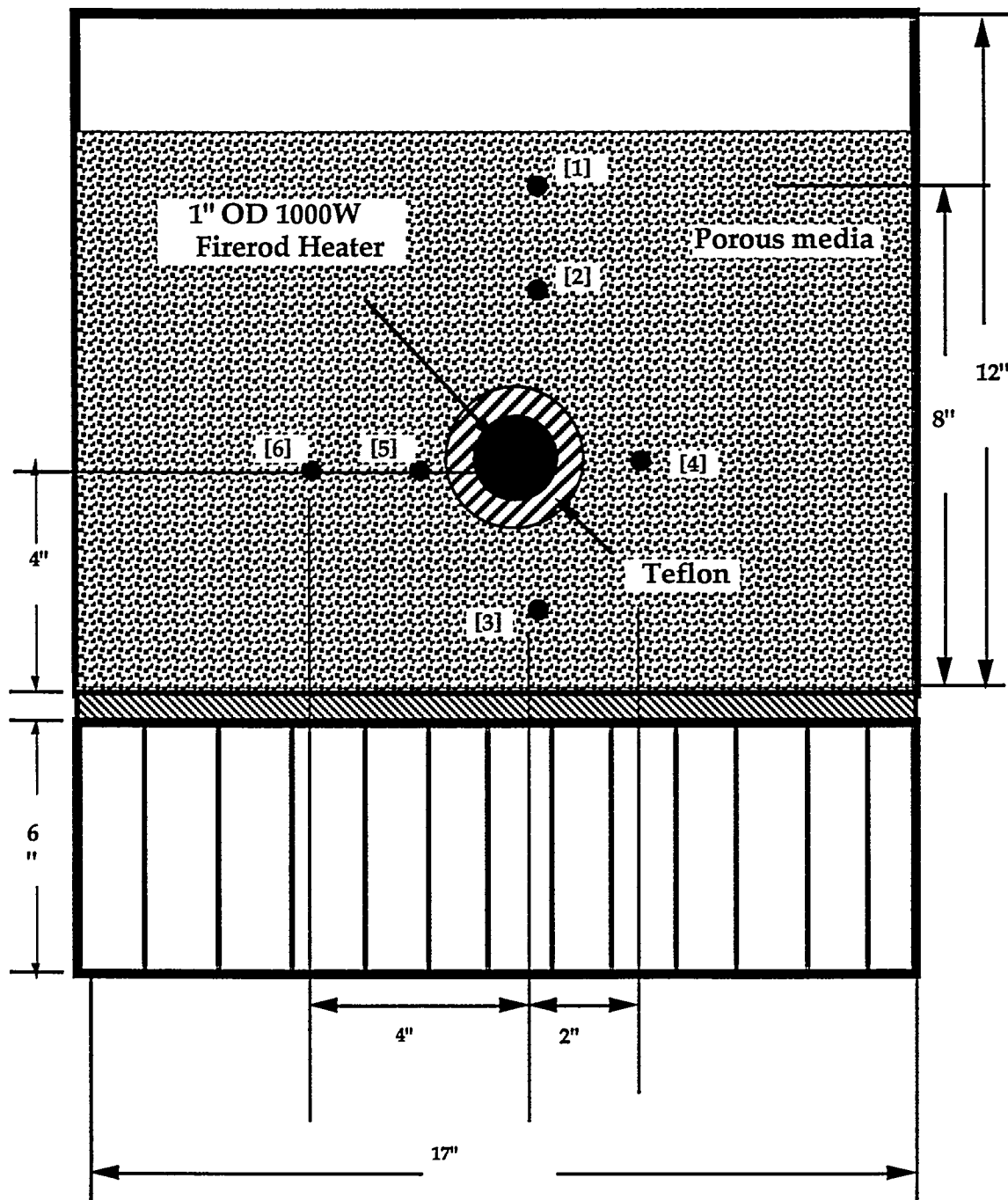


Figure 8. Location of capacitance elements placement in the center plane of the bed via a front view of the apparatus.

Moisture migration in the bed was monitored using capacitance element sensors as a function of time. All of the results for this experiment were reported in the quarterly reports dated November 1, July 20, and April 20, in 1994, and on November 1 and July 20, in 1993. The results include the moisture migration in the porous bed, the amount of water collected in the bottom partitions for both the heated case and the unheated case, analysis of the redistribution effects due to the heater being "on", and the temperature variations of different thermocouples in the porous bed.

#### **IV. Small Experiments Comparing Glass Beads and Silica Gel**

In these experiments, silica gel particles were evaluated as a visualization technique for unsaturated flows. As is well known, silica gel is hygroscopic. In the course of adsorbing water, the silica gel material changes color over a wide range, proportional to the amount of water present. Heat is also liberated when water is adsorbed. The heat of adsorption is a function of gel water content and is the summation of heat condensation and heat of wetting. Hence, the temperatures increase when the water reaches a given location. The amount of heat release from the adsorption phenomena can be significant enough to change the temperature profiles over what would have been indicated from the effects of only the water and heating element. This is clearly a drawback to the technique.

A 12" long x 1" wide x 12" high Plexiglas test section was constructed. 0.0661" diameter silica gel and 0.037" diameter quartz beads were used (separately) as the fill materials. A 1" OD and 1.5" long 500W cartridge heater was used as the heat source. To maintain the temperature of the heater at 180°C, a temperature controller and a variable transformer were used to control the input power. Seventeen 30-gauge type K (chromel-alumel) thermocouples were used in this experiment (see Figure 9 for the placement of these). Polyurethane foam was used as an insulator on all outer surfaces of the test section except the top surface. A predetermined amount of water (this varies from test to test) was uniformly distributed from the top of test cell. Data from the experiment were collected on the LabVIEW data acquisition system. Food coloring was injected in the fill material to try to visualize the flow patterns that might take place. Tap water was used in these experiments, and its initial temperature was 25°C in all cases.

All results for this experiment were reported in the quarterly reports dated July 20 and April 20, both in 1994. The results include the temperature response after the water was admitted uniformly on to the top of the glass-bead-filled test section

and the temperature response after the water was admitted on to the test section filled with the silica gel particles.

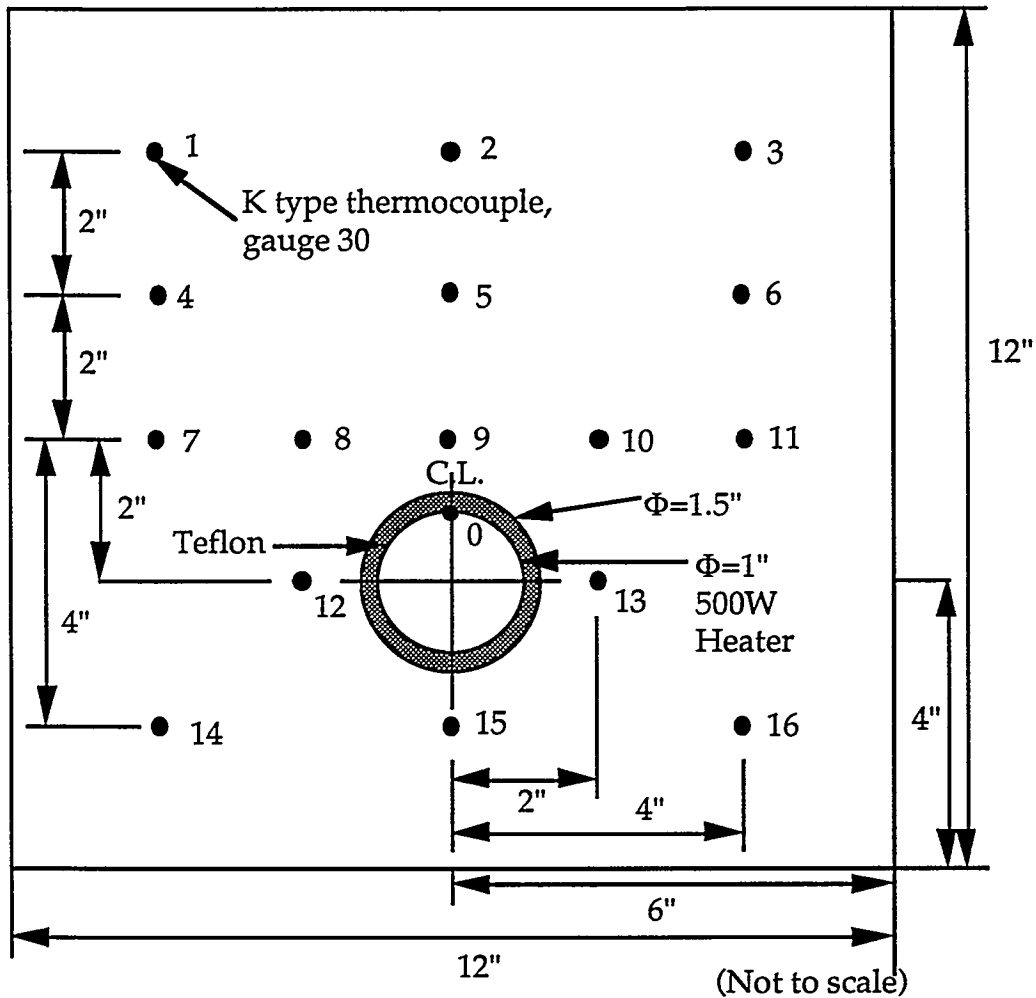


Figure 9. Location of the thermocouples used in the small test section

### V. Small Experiments Comparing Glass Beads and Silica Gel with a "Water Table"

These experiments were closely related to those reported in the section above. In this case, there was an attempt to drive convective currents which would interact with a water layer on the bottom of the test cell.

A 12" long x 1" wide x 12" high Plexiglas test section has been constructed to evaluate the effects of a "water table" on experiments similar to those discussed above. "Water table" in this context refers to a layer of water that remains at the bottom of the apparatus during the complete test. Silica gel beads with an average of 0.0661" diameter and 0.037" diameter quartz beads were used (separately) as the fill materials in these experiments. A 1" OD and 1.5" long 500 W cartridge heater was

used as the heat source. A temperature controller and a variable transformer were used to control the input power to the heater such that the heater temperature could be maintained at 200°C. Thirty 30-gauge type K (chromel-alumel) thermocouples were used in this experiment. Polyurethane foam was used as an insulator on all outer surfaces except the top surface.

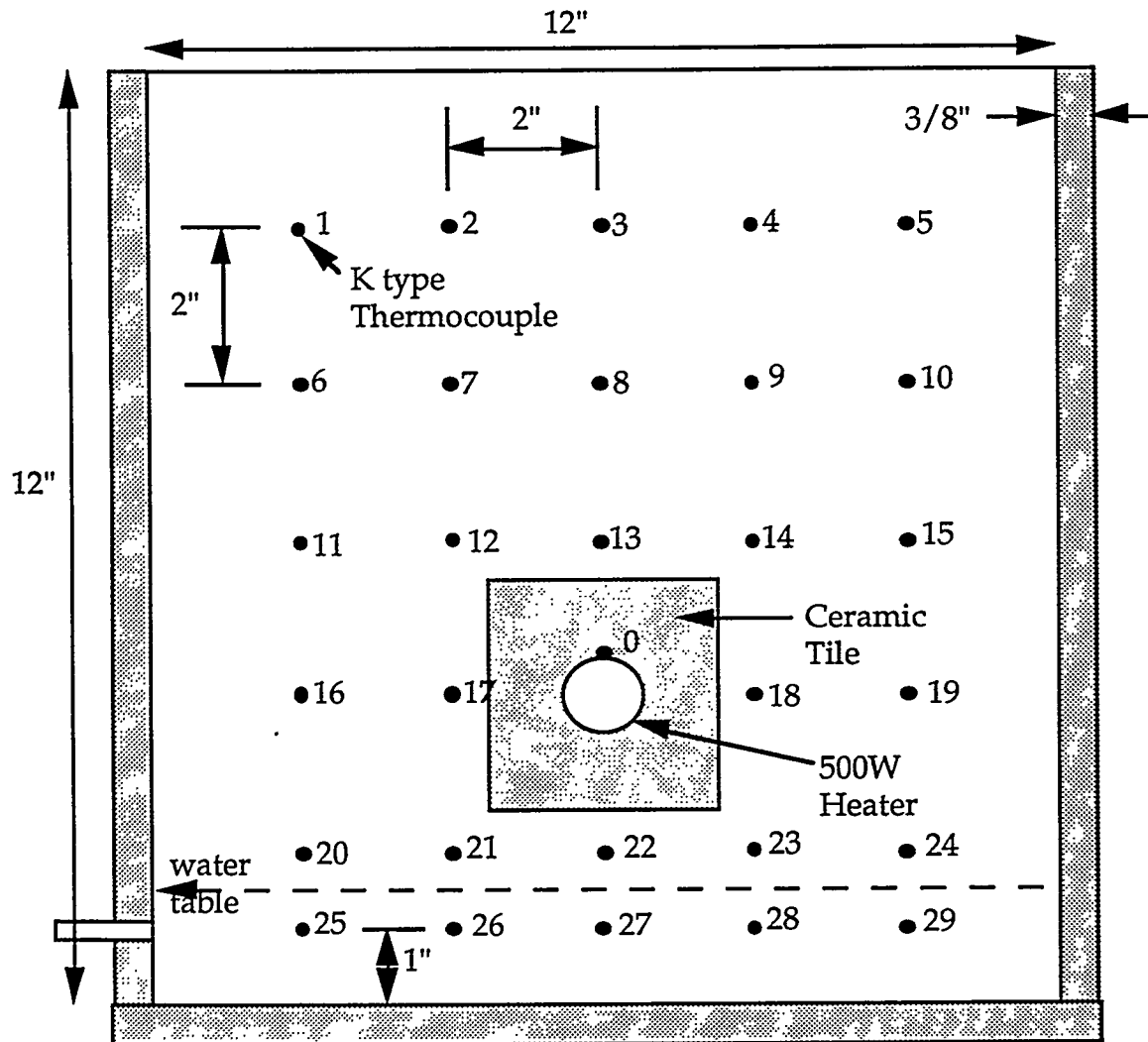


Figure 10. Schematic diagram of the test section for the "water table" experiments.

Sealed and isothermal boundary conditions were used on the top of the test cell, and the isothermal condition was accomplished via an isothermal bath and a custom small heat exchanger. A constant thickness (1.5") water table was maintained on the bottom of the test cell and additional water was added into the test cell as needed to maintain this level. The amount added was noted as part of the data. The LAB View data acquisition system was used to collect experimental

data. Food coloring was used in the glass beads test to try to visualize the flow patterns in the test section. Tap water was used in these experiments, and its initial temperature was 25°C in all cases. Figure 10 shows the schematic of the test section.

All results of this experiment were reported in the quarterly report dated July 20, 1994. This includes the temperature profiles in the porous medium and information about the moisture flows.

## VI. A Study of Christiansen Filters in the Phase Change of Porous Media

A study of the phase change characteristics of Christiansen filters was carried out in order to determine the experimental conditions most favorable to the use of this method. If the optical characteristics of the solid and liquid phases in a saturated porous medium are matched, an optical path through the porous medium would be unimpeded. There is a problem with this approach, however. The dispersion curves of the solid and liquid phases constituting a transparent saturated porous medium generally have different slopes. It is thus impossible to achieve the equality of the refractive indices for all wavelengths simultaneously. For a given temperature, the dispersion curves intersect at a point corresponding to a single wavelength. However, this phenomena can be exploited to perform visualization of temperature fields inside a heat porous medium. Previous studies have been done in saturated media. We had hoped to perform studies in three-phase systems (where a liquid is changing to the vapor phase in a porous medium).

For our investigation, we had hoped to use ethyl salicylate ( $\text{HOC}_6\text{H}_4\text{COOC}_2\text{H}_5$ ) as the liquid phase medium, and perform phase change experiments. It turned out that the boiling point of ethyl salicylate is too high for our purposes (about 233°C). Therefore, it was not a suitable material to do the phase change study in the Christiansen filters.

A suitable liquid phase organic chemical material for our research had to meet the following requirements: its refractive index should be close to 1.51 which is the refractive index of the soda-lime glass beads which we planned to use in the solid phase; the boiling point should not be so high that commercial heaters could provide the energy to evaporate the fluid; it should be non-toxic or have a very low toxicity; it should be a clear and colorless liquid; it should not be reactive with metal, air, and water vapor; it should be non-flammable and non-explosive; stable; and low cost.

We found that tetrachloroethylene ( $\text{Cl}_2\text{C}=\text{CCl}_2$ ) might be a satisfactory material. Its refractive index is 1.509 at 25°C, and the boiling point is 121°C.

A few chemicals have been used in earlier studies of a single phase (i.e. below the boiling points of the organic chemical liquids). For instance, chlorobenzene ( $C_6H_5Cl$ ), has a refractive index of 1.5216 at  $25^\circ C$  and a boiling point of  $131.6^\circ C$  at standard conditions. The volatile and flammable characteristics of chlorobenzene were a disadvantage for our experimental study. Its vapor is also very harmful. Benzyl alcohol ( $C_6H_5CH_2OH$ ) has a refractive index about 1.5385-1.5405 at  $20^\circ C$  and a boiling point about  $206^\circ C$ . The latter ruled out this substance for our application. Nitrobenzene ( $C_6H_5NO_2$ ) is a yellow, oily liquid and poisonous. The mixture of carbon disulfide ( $CS_2$ ) and acetone ( $CH_3COCH_3$ ) has also been used in the Christiansen filter experiments in the past years. The boiling point of this mixture liquid is very low (about  $50^\circ C$ ) but carbon disulfide is a very poisonous and extremely flammable chemical to be used in the phase change study. In addition, acetone is also a extremely flammable liquid. Benzene ( $C_6H_6$ ) has a refractive index of about 1.515-1.517 and a boiling point about  $80.1^\circ C$ . Because it has been proved to be carcinogenic, toxic, narcotic, as well as extremely flammable and poisonous, we decided to avoid using it. Anisole or methylphenyl ether ( $C_6H_5OCH_3$ ), bromotrichloromethane ( $CCl_3Br$ ), n-butyl phenyl acetate ( $C_4H_9OOCH_2C_6H_5$ ), isopropyl iodide ( $CH_3CH_2CH_2I$ ), mercaptoethanol ( $HSCH_2CH_2OH$ ), para-methyl anisol ( $CH_3C_6H_4OCH_3$ ), methyl benzoate ( $C_6H_5CO_2CH_3$ ), ethyl iodide ( $CH_3CH_2I$ ), glycol dimercaptopropionate ( $HSCH_2CH_2COOCH_2$ )<sub>2</sub>, para-chlorotoluene ( $ClC_6H_4CH_3$ ), cuminic alcohol ( $CH_2OH C_6H_4CH(CH_3)_2$ ), and 1-phenyl butene-2 ( $C_6H_5CH_2CH=CHCH_3$ ) have broadly been studied and investigated in our research and we could not find a suitable chemical other than tetrachloroethylene.

We found that the transmission coefficient of a Christiansen light filter is an exponential function which involves five important variables; (a) the wavelength of the light, (b) the thickness of the cell, (c) the size of the individual particles of the powder, (d) the difference between the refractive indices of the powder and the surrounding liquid, and (e) the proportions of the volume of the cell occupied respectively by the liquid and by the particles of the powder. Thus, we needed a tunable laser to give us a variety of wavelengths to correspond to the equality of refractive indices when we heat the cell up until the liquid's boiling point. We have gotten only a few satisfactory figures of wavelength versus refractive index at the different temperatures on our 5 W argon-ion laser which could cover all the wavelengths.

The experiments to determine the wavelength corresponding to the equality of the refractive indices and how that varies with the temperatures have been

accomplished via a calibration setup. This was done with a 2 inch-diameter test cell filled with 2 mm-diameter soda-lime glass beads. The index of refraction of a fluid is a function of both its temperature and the wavelength of the incident light; whereas, the index of refraction of the solid (glass) is primarily a function of the wavelength of the incident light and only very weakly a function of temperature. Thus, if a temperature gradient exists in the porous medium which is perpendicular to the optical axis (of the incident light), various wavelengths of light will penetrate the test section at different locations. This situation arises because the indices of refraction of the fluid and the solid medium match at one wavelength for a particular temperature.

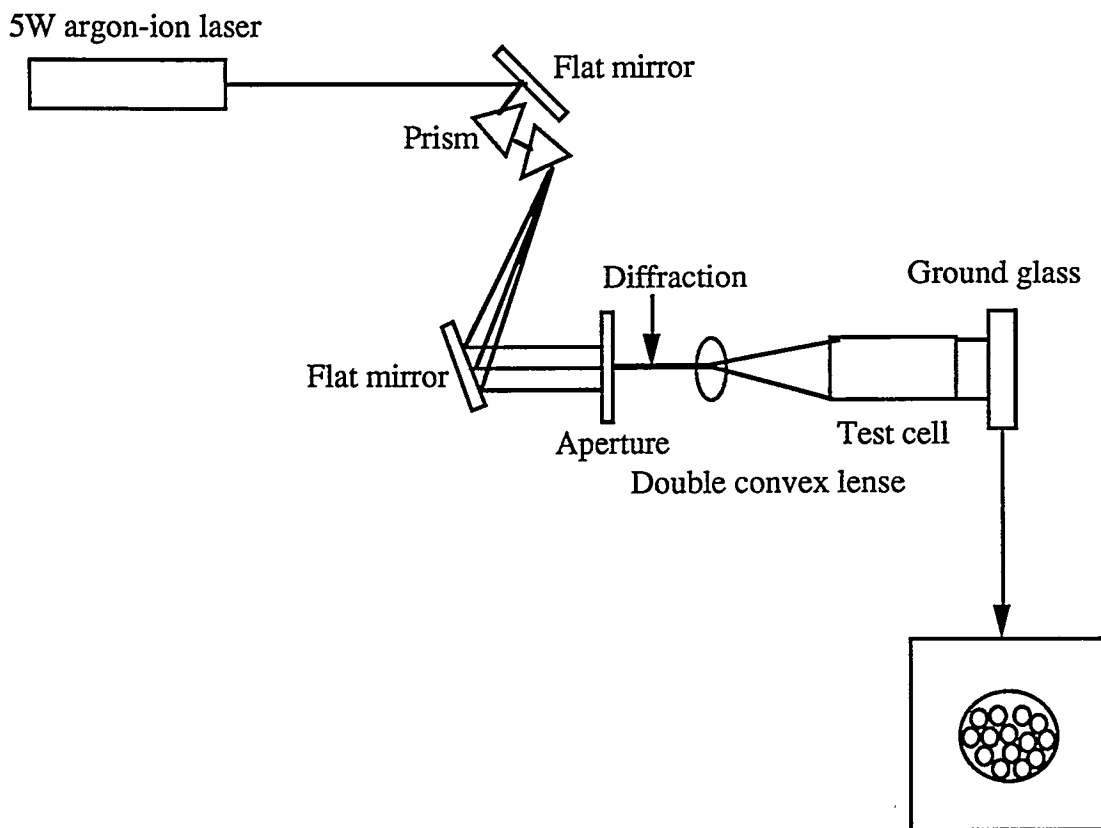


Figure 11. The schematic diagram of the optical setup.

A gauge 30 K type thermocouple was placed at the center of the test cell. An Omega thermocouple thermometer was used to indicate the temperature from the thermocouple. Insulation was used to cover the test cell (except for the viewing area). The organic chemical liquid and glass beads were heated up by a band heater that was placed inside the insulation and outside the test cell. A variable voltage transformer was used to control the input power to the heater, which in turn

controlled the temperature of the test cell. The image of glass beads was then found at a certain temperature and wavelength where refractive indices matched. The schematic diagram of the optical setup is shown in Figure 11.

All of the results for this experiment have been reported in the quarterly reports dated July 20 and November 1, 1993, and January 20, April 20, and July 20, 1994. The results given in these reports include the correspondence between temperature and wavelength for the soda-lime glass beads and chlorobenzene. The governing theoretical equations are also summarized.

#### **DISCLAIMER**

This report was prepared as an account of work sponsored by an agency of the United States Government. Neither the United States Government nor any agency thereof, nor any of their employees, makes any warranty, express or implied, or assumes any legal liability or responsibility for the accuracy, completeness, or usefulness of any information, apparatus, product, or process disclosed, or represents that its use would not infringe privately owned rights. Reference herein to any specific commercial product, process, or service by trade name, trademark, manufacturer, or otherwise does not necessarily constitute or imply its endorsement, recommendation, or favoring by the United States Government or any agency thereof. The views and opinions of authors expressed herein do not necessarily state or reflect those of the United States Government or any agency thereof.